Proceedings of the
Annual Stability Conference
Structural Stability Research Council
Charlotte, North Carolina, April 11-14, 2022

Shear buckling coefficients for longitudinally stiffened-haunched steel plate girders

Pablo Rico[1], Mariana Echeverri[2], Carlos Graciano[3]

Abstract

In this paper, the critical buckling behavior of haunched steel plate girders subjected to shear loading is investigated in depth. The study is conducted through linear buckling analysis using the finite element method. First, the results are validated with previous results for simply supported rectangular and nonrectangular web panels. Thereafter, an extensive parametric study is conducted to investigate the influence of various geometric parameters including the inclination angle, the panel aspect ratio, the size of the flanges and the presence of longitudinal stiffeners on the buckling coefficients. Finally, the results are employed to develop expressions for the shear buckling coefficients for longitudinally stiffened-haunched steel plate girders taking into account the forementioned parameters.

1. Introduction

In modern construction, sustainability has become an important factor in structural design. In sustainable design, the use of traditional materials is optimized or new materials are employed. In this sense, girder with haunches, also called tapered girders or nonrectangular panels, are increasingly employed particularly in the design of steel bridges curved in elevation. In this case, the girder depth is reduced from intermediate supports (maximum depth) to mid span (minimum depth). Over the last decades, tapered girders have been the focus of several research projects, nevertheless this paper is aimed at analyzing tapered plate girder subject to shear.

Usually, two types of analysis are performed to investigate the shear response of tapered steel girders, ultimate strength analysis and linear buckling analysis. The shear strength of unstiffened tapered girder webs has been investigated experimentally and numerically (Mirambell and Zarate 2000, Zarate and Mirambell 2004, Real et al. 2010, Bedynek et al. 2013, Bedynek 2014, Bedynek et al. 2017, Ibrahin et al. 2020, Sediek et al. 2020). The effect of longitudinal stiffening on the shear strength of tapered plate girders was also investigated (Bedynek et al. 2013, Bedynek 2014). Compared to flat web plates, corrugated plates offer an enhanced out-of-plane stiffness that can increase the shear strength of tapered girders (Hassanein and Kharoob 2014, Hassanein and

[1] Graduate Research Assistant, Universidad Nacional de Colombia, <pricog@unal.edu.co>
[2] Undergraduate student, Universidad Nacional de Colombia, <mecheverrilo@unal.edu.co>
[3] Full Professor, Universidad Nacional de Colombia, <cagracianog@unal.edu.co>

Kharoob 2015, Zevallos et al. 2016). Linear buckling analyses of unstiffened tapered web girder have also been performed (Bedynek et al. 2013, Bedynek et al. 2014, Ibrahim et al. 2020; AbdelAleem et al. 2022). In these linear analyses, the influence of the girder flanges was disregarded.

Recently, the strength of longitudinally stiffened tapered girder web panels subjected to combined bending and shear was investigated experimentally and numerically (Poroustad and Kuhlmann 2018, Poroustad and Kuhlmann 2018, Kuhlmann et al. 2020, Poroustad and Kuhlmann 2021). In these studies, the tapered girders had one horizontal flange and an inclined one, and the longitudinal stiffener was placed either parallel to the upper or lower flange. Furthermore, in the loading protocol the inclined flange was always under compression.

As seen above, there is a still a need to investigate the critical buckling response of longitudinally stiffened-haunched girders subject to shear. Therefore, this paper aims at investigating the linear buckling response of this type of girders. The study in conducted numerically through linear buckling analysis using the finite element method. Firstly, a numerical model is built for simply supported rectangular panel subject to shear loading. Once the model is validated, the geometry is extended to longitudinally stiffened-haunched girders. After that, a parametric analysis is performed to investigate the influence of various geometric variables including the inclination angle, the panel aspect ratio, the size of the flanges and the presence of longitudinal stiffeners on the buckling coefficients. In the end, the results from the parametric study are employed to develop expressions for the shear buckling coefficients for longitudinally stiffened-haunched steel plate girders.

2. Numerical modeling

Fig. 1 shows the nomenclature used herein for longitudinally stiffened-haunched plate girders. A finite element model is developed using the software ANSYS (ANSYS 2022). Shell 181 elements, with four nodes and six degrees of freedom on each node are employed to model the girder components (flanges, web and stiffener). A unit load is applied downward in the web at the lower height end, as shown in Fig. 2. Through eigenvalue buckling analysis, critical buckling stresses τ_{cr} are computed, and according to the theory of plates stability, buckling coefficients are obtained. The critical buckling shear stress for a simply supported rectangular plate is expressed as

$$\tau_{cr} = k_s \frac{\pi^2 E}{12(1-\nu^2)} \left(\frac{t_w}{h}\right)^2 \quad (1)$$

where k_s is the shear buckling coefficient, E is the modulus of elasticity, ν is the Poisson's ratio, h is the web depth, and t_w is web thickness.

2.1 Geometry and parameters

Table 1 presents the variables and their range for the parametric study. This geometry is intended to recreate the behavior of haunched girders near the supports of bridges, in which the inclined flange is under compression and the tension field is developed in the short diagonal. Through the analysis, the longitudinal stiffener is always located from mid height of the lower end (h_0 /2), and varies its inclination: horizontal, parallel to the inclined flange, and from mid-height (h_1 /2) to mid-height (h_0 /2).

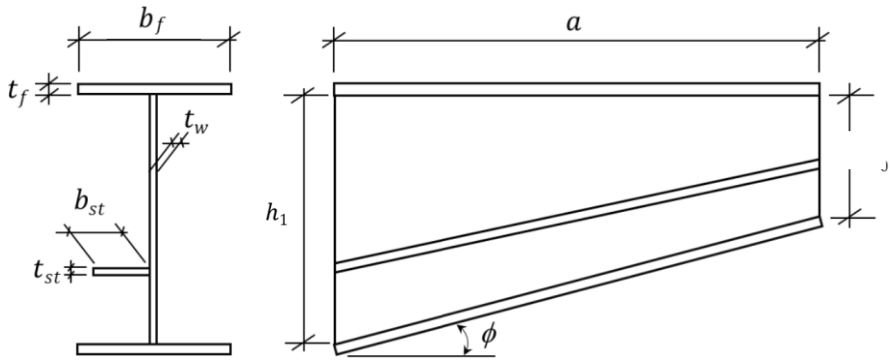

Figure 1: Geometry of longitudinally stiffened-haunched plate girder (Nomenclature)

Table 1: Parameters

Parameters	
Dimension	Value
h_0 [mm]	1000
b_f	$h_1/6$
ϕ [°]	0, 10, 15, 20, 30
a/h_0	1, 2, 3
h_1/t_w	150, 200, 300
t_f/t_w	1, 2, 3
γ_s	0, 10, 20, 60, 150
Stiffener position	Horizontal, Inclined, Mid-Height
E [MPa]	210000
ν	0.3

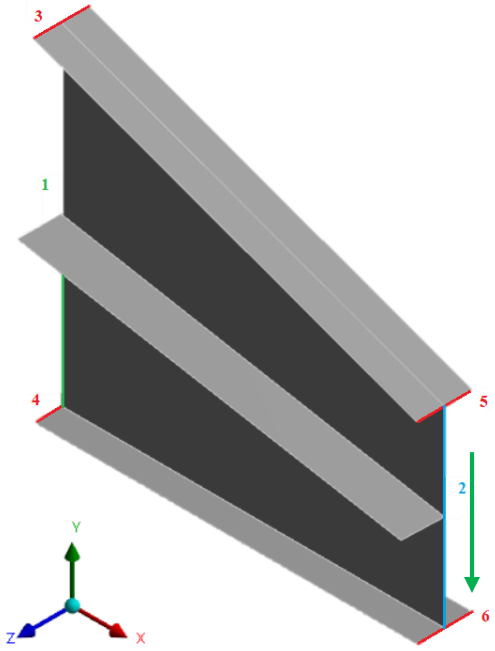

Figure 2: Boundary conditions.

The boundary conditions are shown in Fig. 2 and Table 2. The load is applied downward at the web in the lower end. With this configuration, the tension field is developed in the short diagonal and the inclined flange is under compression.

Table 2: Boundary conditions

Location	Degree of freedom						
	U_x	U_y	U_z	R_x	R_y	R_z	Force
1	R	R	R	R	F	R	0
2	F	F	R	R	F	R	$-U_y$
3, 4, 5, 6	F	F	R	R	R	F	0

*F denotes free and R denotes restrained

2.2 Validation procedure

The following material properties were used throughout the study: E= 210000 MPa and v = 0.3. A mesh converge analysis was conducted in Fig. 3 for an unstiffened girder with small flanges, with the following dimensions $a/h_0 = 1$, $\phi = 15°$, $h_1/t_w = 150$, and $t_f/t_w = 1$. As seen in Fig. 4, the variation in the buckling coefficient is small when for element sizes of 40 mm, hence this element size is chosen for further analysis.

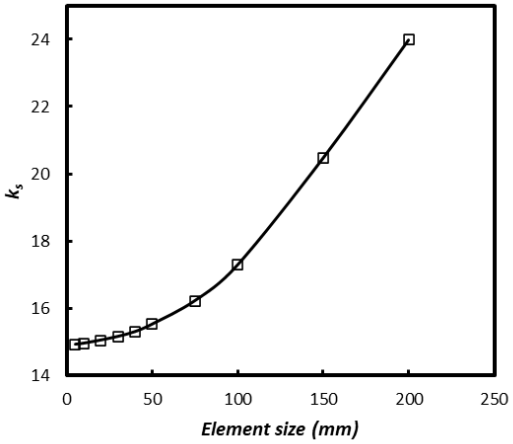

Figure 3. Mesh convergence analysis

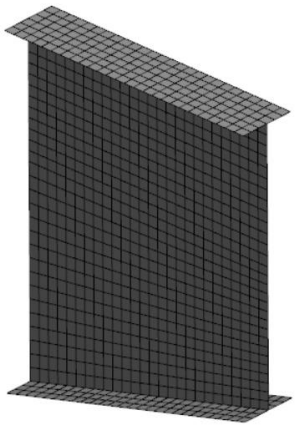

Figure 4. Final mesh

In the literature (Timoshenko and Gere 1936, Ziemian 2010), the shear buckling coefficient for a simply supported rectangular plate subjected to shear is

$$k_s = 5.34 + 4\left(\frac{h}{a}\right)^2 \tag{2}$$

Also, for non-rectangular simply supported plates, (Bedynek, 2013) proposed four different equations depending on the geometry of the plate and loading direction. For a girder with the inclined flange under compression and the diagonal tension field developed in the short diagonal,

$$k_s = 5.5\left(\frac{a}{h_w}\right)^{0.8}\tan(\Phi) + 8.7\left(\frac{a}{h_w}\right)^{-0.8} \tag{3}$$

An additional validation is conducted as follows considering a simply supported plate, with dimensions $a/h_0 = 2$, and $h_1/t_w = 200$. Table 3 presents a comparison between the shear buckling coefficients computed through the finite element model and the those obtained with Eqs. (2) and (3). It is worth pointing out that the value used for h in Eq. (2) is the major height $h=h_1$.

Table 3: Model validation

Φ	k_s^{FEM}	$k_s^{Eq.(2)}$	$k_s^{Eq.(3)}$	k_s^{FEM} / $k_s^{Eq.(2)}$	k_s^{FEM} / $k_s^{Eq.(3)}$
0	6.67	6.34	6.59	1.05	1.01
5	8.08	7.17	8.77	1.13	0.92
10	8.78	7.70	9.65	1.14	0.91
20	9.48	8.33	10.46	1.14	0.91
30	10.97	9.98	11.95	1.10	0.92

According to the presented results, with differences between the model and the literature of less than 15%, the model is then validated.

3. Parametric study

For the sake of generalization, the effect of five variables in the shear buckling coefficient is studied. The variables are: The flexural rigidity of the stiffener γ_s, the web slenderness h_1/t_w, the ratio of flange thickness to web thickness t_f/t_w, the aspect ratio a/h_0 and the haunch inclination $tan(\Phi)$. The different values of the parameters are shown in Table 1, resulting in 2025 cases to run. The analysis of the results is presented next.

3.1 Influence of the stiffener position and flexural rigidity γ_s

The stiffener flexural rigidity is defined as:

$$\gamma_s = 10.9 \frac{I_{st}}{h_w {t_w}^3} \tag{4}$$

where I_{st} is the second moment of area of the stiffener respect to an axis placed at the centroid of the area including the stiffener and a portion of the web of $15t_w$ on each side as defined by the Eurocode (EC3, 2006). This code also states that when calculating the shear buckling coefficient, the value of the second moment of area must be divided by three.

Fig. 5 shows the variation of the buckling coefficient k_s in terms of γ_s. The main analysis is that after a reaching a certain value of γ_s, there is not a significant increase of the value of k_s. This value is the transition between the behavior of a weak stiffener and the behavior of a strong stiffener. As presented in the previous plots, the value of minimum rigidity for a strong stiffener is $\gamma_s=20$. After this value the buckling coefficient remain almost constant, therefore the conclusion is that for a strong stiffener, there is no influence of the flexural rigidity on the value of k_s. Subsequently, the following analyses are performed using only strong stiffeners.

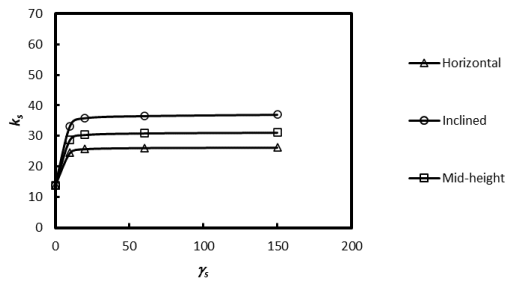

(a) $\phi = 10°$

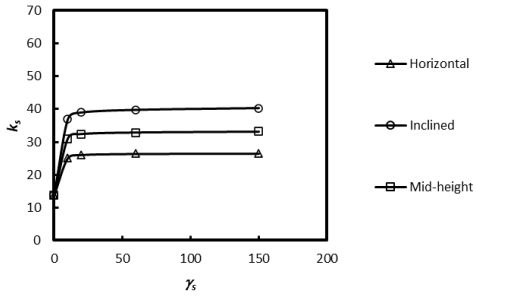

(b) $\phi = 15°$

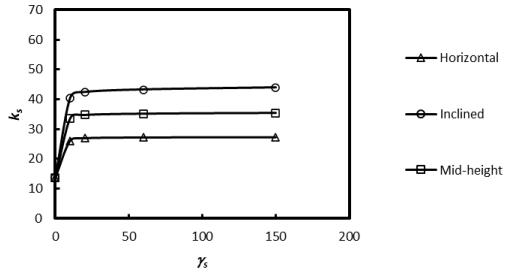

(c) $\phi = 20°$

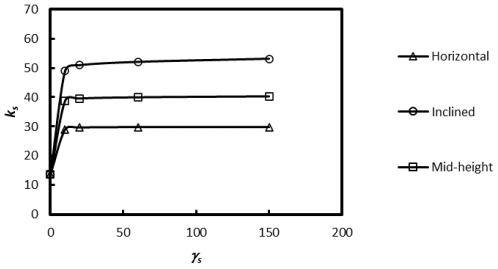

(d) $\phi = 30°$

Figure 5: Buckling coefficients k_s in terms of γ_s (a/h_0=1, h_1/t_w =300, t_f/t_w=1).

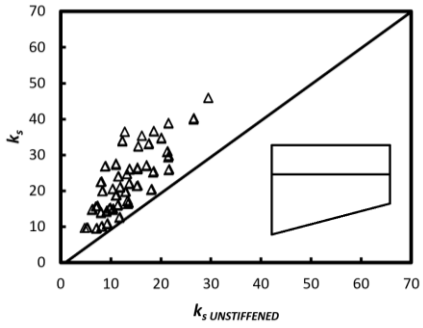

(a) Horizontal stiffener

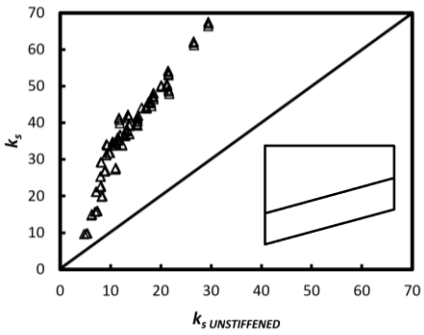

(b) Inclined stiffener

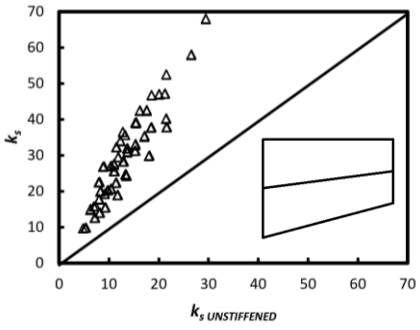

(c) Mid-height stiffener

Figure 6: Influence of the stiffener placement.

Fig. 6 shows a significant enhancement in the buckling coefficient with the usage of a longitudinal stiffener. On average, the use of a strong horizontal stiffener increases k_s by a 78% (Fig. 6a). A

strong stiffener placed parallel to the inclined flange increases k_s on the average by a 179% (Fig. 6b), and a strong stiffener placed at both of mid heights increases k_s by a 124% (Fig. 6c).

3.2 Influence of the web slenderness h_1/t_w

Fig. 7 shows the variation of k_s with respect to the web slenderness h_1/t_w, for γ_s =150, a/h_0=2 and t_f/t_w=2.

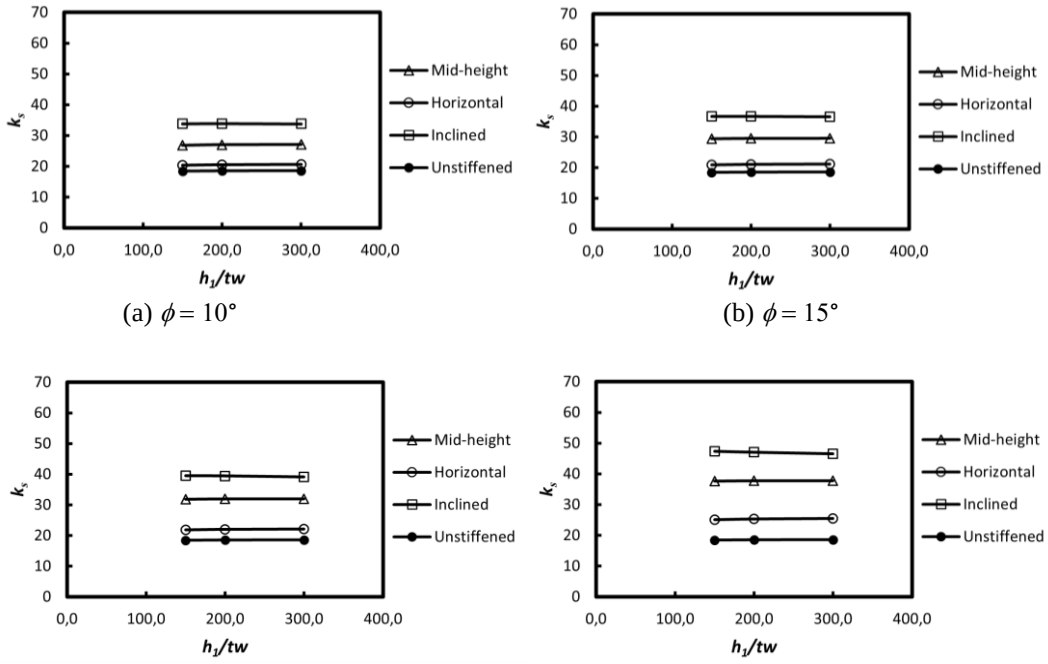

(a) $\phi = 10°$ (b) $\phi = 15°$

(c) $\phi = 20°$ (d) $\phi = 30°$

Figure 7: Buckling coefficients k_s in terms of h_1/t_w (γ_s =150, a/h_0=2, t_f/t_w=2)

It is clearly observed that the slenderness parameter h_1/t_w has a diminished impact on the shear buckling coefficient, as long as the web is slender $h_1/t_w > 150$ and the code limit is maintained $h_1/t_w < 300$ (AASHTO 2020). For this reason, the following results will not include the aforementioned parameter.

3.3 Influence of the thickness ratio t_f/t_w

From Fig. 8 to Fig. 11 the variation of buckling coefficient k_s in terms of t_f/t_w is shown.

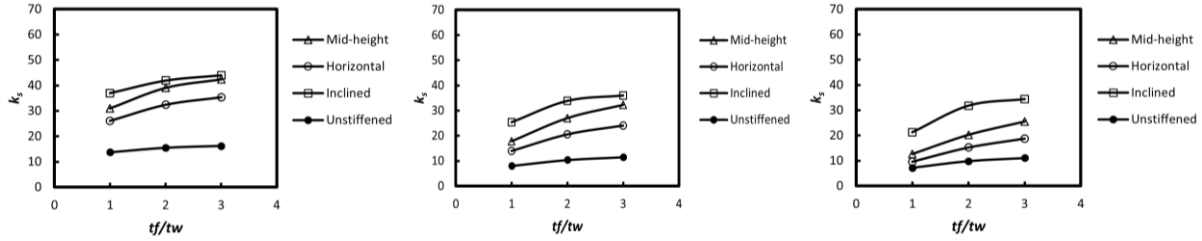

(a) a/h_0=1 (b) a/h_0=2 (c) a/h_0=3

Figure 8: Buckling coefficients k_s in terms of t_f/t_w (γ_s = 150, $\phi = 10°$)

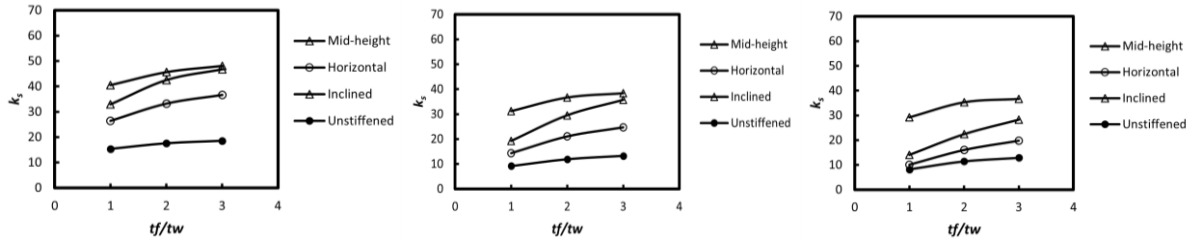

(a) a/h_0=1 (b) a/h_0=2 (c) a/h_0=3

Figure 9: Buckling coefficients k_s in terms of t_f/t_w (γ_s =150, ϕ = 15°)

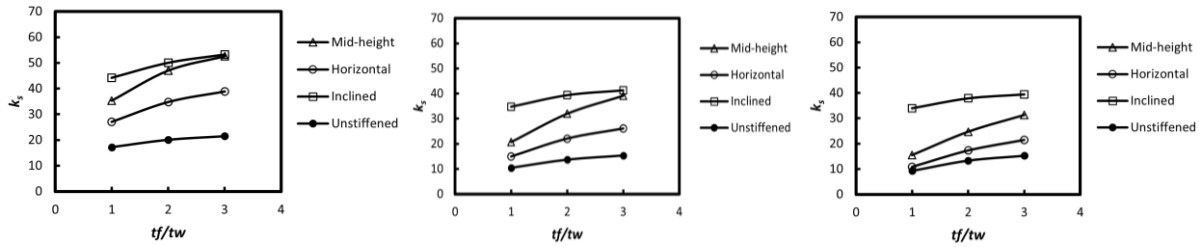

(a) a/h_0=1 (b) a/h_0=2 (c) a/h_0=3

Figure 10: Buckling coefficients k_s in terms of t_f/t_w (γ_s =150, ϕ = 20°)

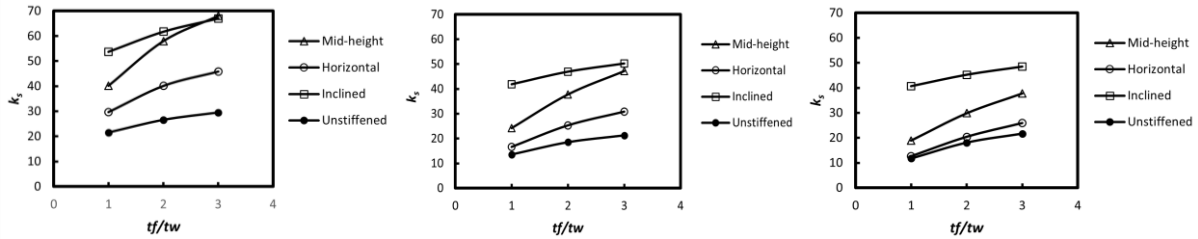

(a) a/h_0=1 (b) a/h_0=2 (c) a/h_0=3

Figure 11: Buckling coefficients k_s in terms of t_f/t_w (γ_s =150, ϕ = 30°)

It is observed that for all cases, there is an increase in the buckling coefficient as the flange-to-web thickness ratio is greater. This is expected, as the thickness of the flanges increase, the boundary condition of the web to flange juncture approaches to a fixed support, thus increasing the rigidity and the shear capacity of the girder. As the variation of this ratio makes the buckling coefficient change, this value is included in the analysis.

3.4 Influence of the panel aspect ratio a/h_0

From Fig. 12 to Fig. 15, the variation of the buckling coefficient k_s in terms of the aspect ratio a/h_0 is presented.

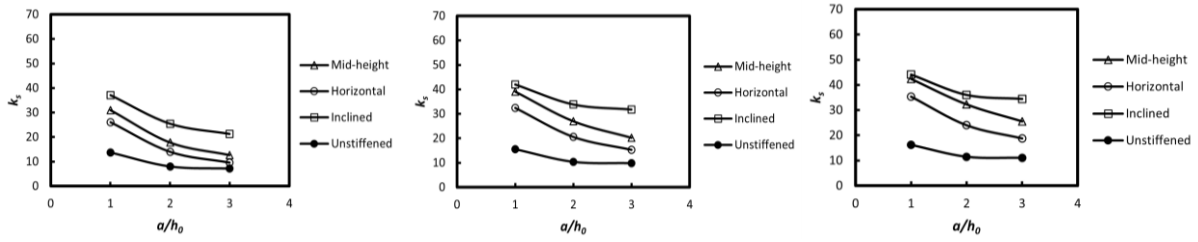

(a) t_f/t_w=1 (b) t_f/t_w=2 (c) t_f/t_w=3

Figure 12: Buckling coefficients k_s in terms of a/h_0 (γ_s =150, ϕ = 10°)

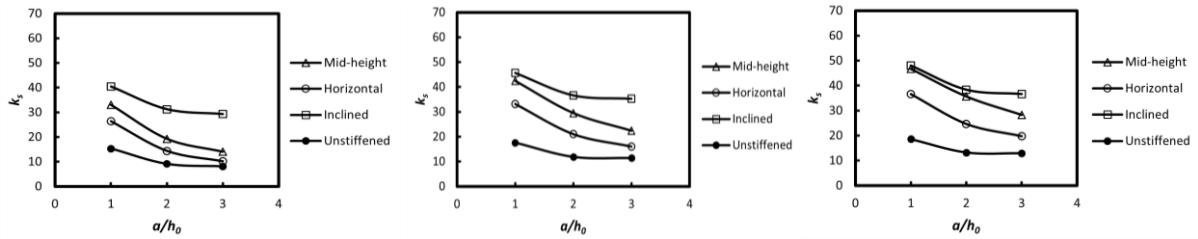

(a) t_f/t_w=1 (b) t_f/t_w=2 (c) t_f/t_w=3

Figure 13: Buckling coefficients k_s in terms of a/h_0 (γ_s =150, ϕ = 15°)

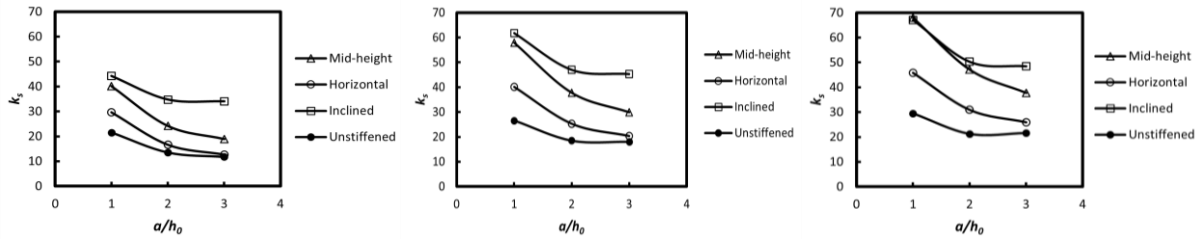

(a) t_f/t_w=1 (b) t_f/t_w=2 (c) t_f/t_w=3

Figure 14: Buckling coefficients k_s in terms of a/h_0 (γ_s =150, ϕ = 20°)

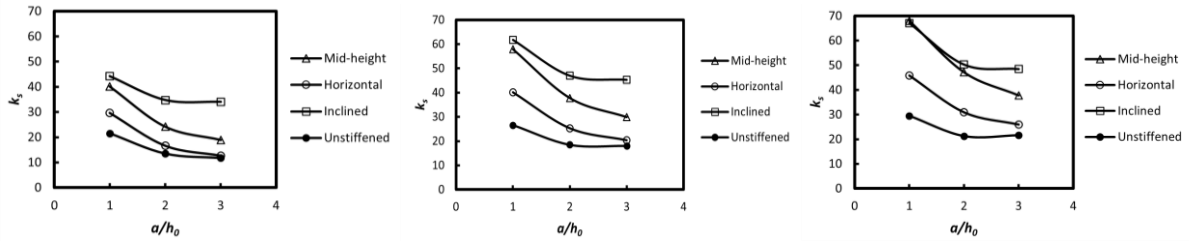

(a) t_f/t_w=1 (b) t_f/t_w=2 (c) t_f/t_w=3

Figure 15: Buckling coefficients k_s in terms of a/h_0 (γ_s =150, ϕ = 30°)

It is observed that for all cases, as the aspect ratio increases, the buckling coefficient decreases. This is explained because as the panel aspect ratio increases, the panel is longer and bending stresses increase, thus reducing shear buckling capacity. As this parameter makes the buckling coefficient change, this value must be included in the analysis.

3.5 Influence of the haunch inclination tan(ϕ)

From Fig. 16 to Fig. 18 the variation of the buckling coefficient in terms of the haunch inclination *tan(ϕ)* is presented.

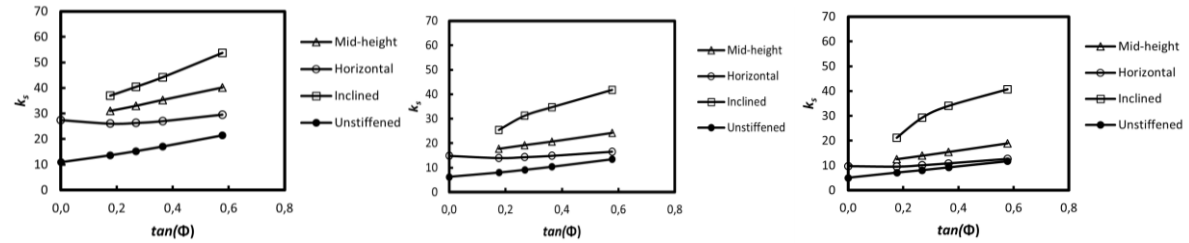

(a) a/h_0=1 (b) a/h_0=2 (c) a/h_0=3

Figure 16: Buckling coefficients k_s in terms of *tan(ϕ)* (γ_s =150, t_f/t_w=1)

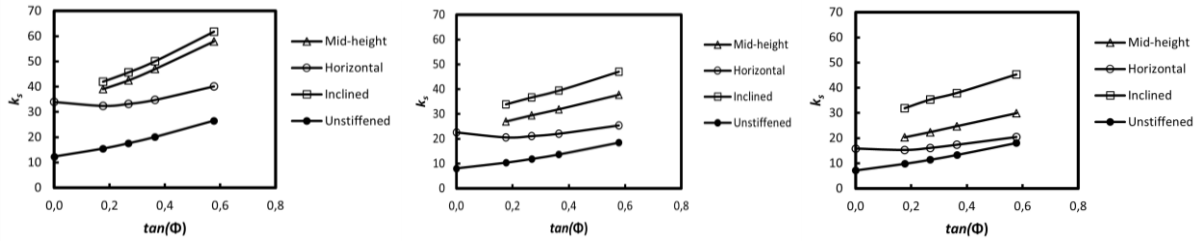

(a) a/h_0=1 (b) a/h_0=2 (c) a/h_0=3

Figure 17: Buckling coefficients k_s in terms of $tan(\phi)$ (γ_s =150, t_f/t_w=2)

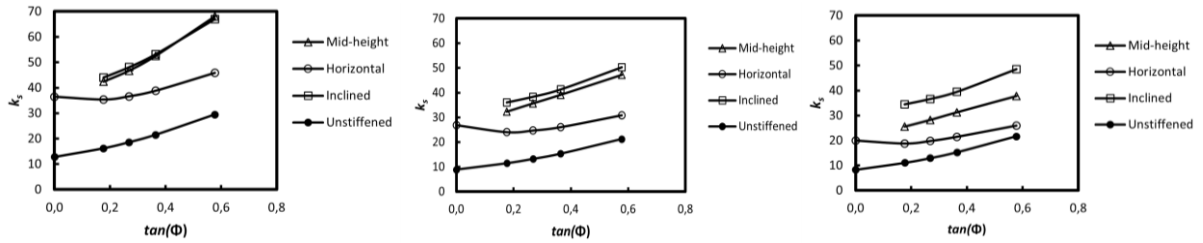

(a) a/h_0=1 (b) a/h_0=2 (c) a/h_0=3

Figure 18: Buckling coefficients k_s in terms of $tan(\phi)$ (γ_s =150, t_f/t_w=3)

It is observed that for all cases, as the haunch angle ϕ increases the buckling coefficient also increases. As this parameter affects the buckling coefficient, this value must be included in the analysis.

3.5 Buckling shapes.

Fig. 19 shows the buckling shapes, varying the stiffener rigidity and position, for a girder with a/h_0=2, t_f/t_w=2, h_1/t_w = 200, ϕ = 20°. Observing the deformed shapes in Fig. 19, the following findings are highlighted:

1. When the panel is unstiffened γ_s= 0, the buckling shape involves the whole web panel, thus reducing the capacity (k_s = 13.70).
2. When the stiffener is weak γ_s = 10, the stiffener does not provide a nodal line of near zero out-of-plane displacement, and the buckling also involves the whole web panel and the stiffener. Nevertheless, the buckling coefficient k_s increases compared to the unstiffened girder.
3. When the stiffener is strong, γ_s = 20, buckling occurs only in the larger sub-panel, as the stiffener restricts the out-of-plane displacement similar to a nodal line with near zero displacements, thus dividing the whole webpanel into two sub-panels, and increasing the capacity of the girder to resisting shear buckling. For γ_s = 150 the difference in the buckling coefficient is very small compared to that obtained for a stiffener with γ_s = 20

γ_s	Stiffener position			
	Unstiffened	Horizontal	Inclined	Mid-Height
10	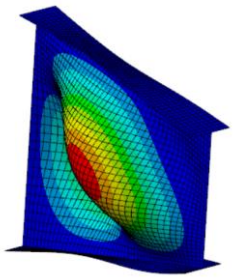 k_s = 13.70	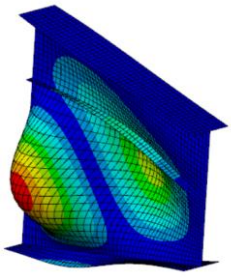 k_s = 20.21	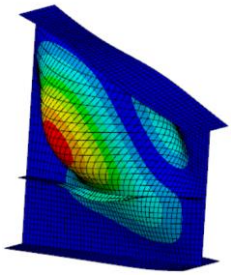 k_s = 33.23	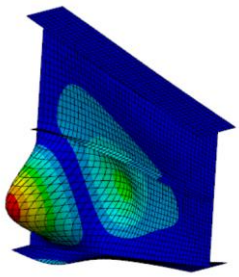 k_s = 30.44
20	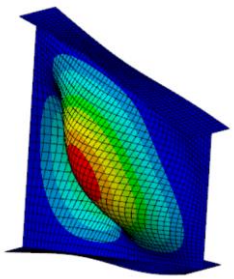 k_s = 13.70	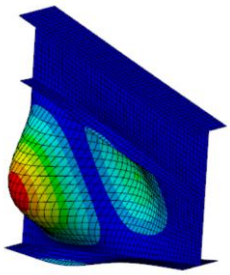 k_s = 21.65	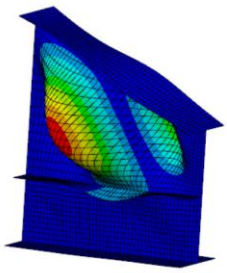 k_s = 37.45	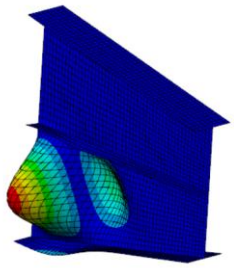 k_s = 31.45
150	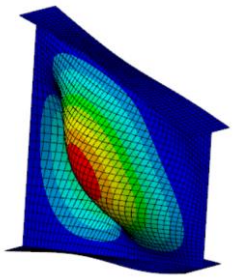 k_s = 13.70	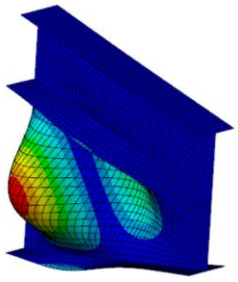 k_s = 22.06	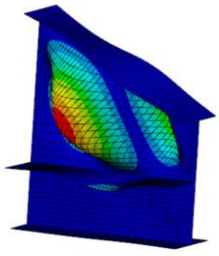 k_s = 39.44	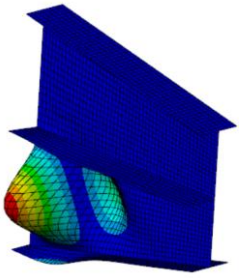 k_s = 31.96

Figure 19: Buckling shapes for a/h_0=2, t_f/t_w=2, h_1/t_w = 200, $\phi = 20°$.

4. Proposal of buckling coefficient

4.1 Procedure

The following procedure was used to develop the prediction models for each of the stiffener positions: horizontal, inclined and Mid-Height.

1. Determine the variables that may influence in the estimation of the buckling coefficient. The selected variables were: t_f/t_w, a/h_0 and $tan(\phi)$. It was found that the influence of the web slenderness ratio, h_1/t_w, can be neglected.
2. It was established that all the equations were going to be set for strong stiffeners.
3. Construct the dependence charts, for all the possible combinations of angles and t_f/t_w, it revealed the relationships between the aspect ratio a/h_0 and the buckling coefficient.
4. Once the trendlines of the charts were established, in the form $y(x)=C_o(x)^{\alpha}$, where $y(x)$ corresponds to the buckling coefficient and (x) to the aspect ratio, the coefficients were tabulated (C_o vs α).
5. The relationship between C_o and α with the parameter $tan(\phi)$ were found plotting them again as shown from Fig. 20 to Fig. 22.

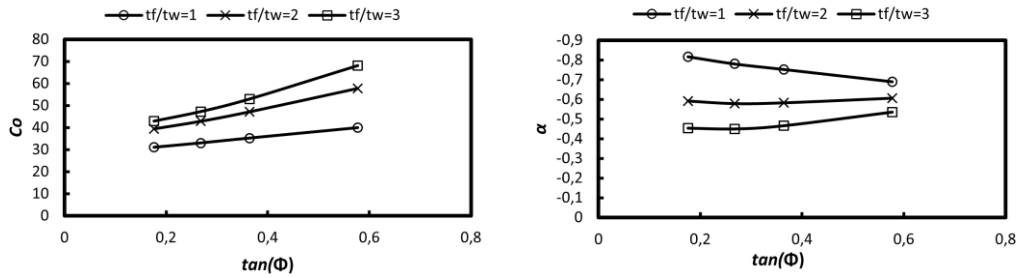

Figure 20: C_o and α in terms of $tan(\phi)$ for Mid-Height position.

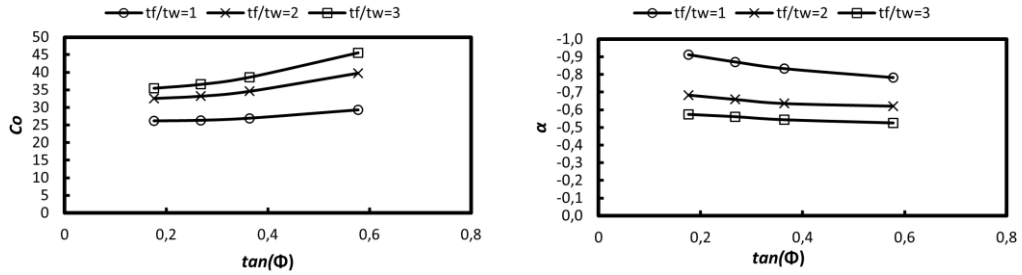

Figure 21: C_o and α in terms of $tan(\phi)$ for horizontal position.

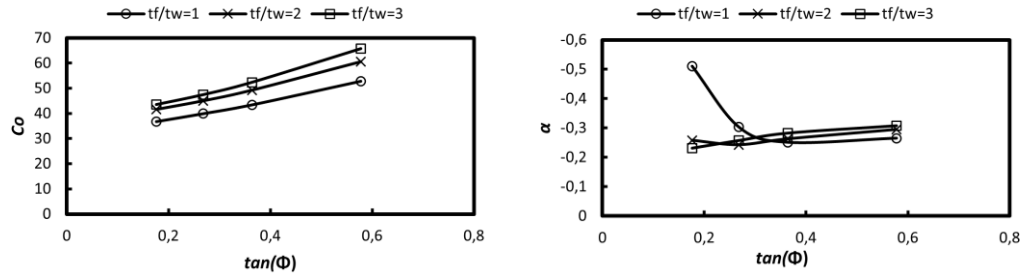

Figure 22: C_o and α in terms of $tan(\phi)$ for inclined position.

6. Polynomial trendlines were made again to fit the formulas that describe C_o and α.
7. A new set of variables a and b were plotted in terms of thickness ratio t_f/t_w, in order to involve all the parameters affecting the buckling coefficient. The plots are shown from Fig. 23 to Fig. 25.

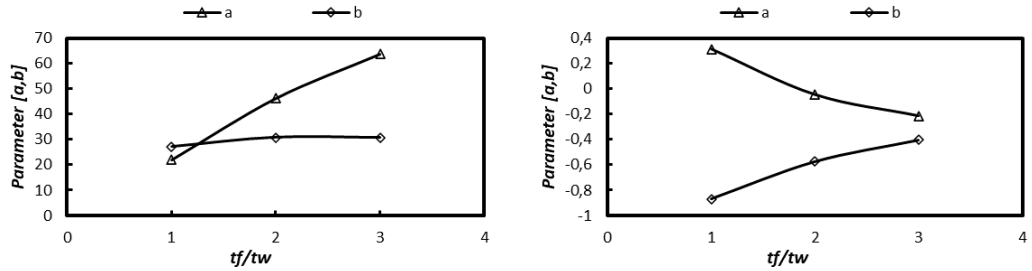

Figure 23: a and b in terms of t_f/t_w for mid-height position.

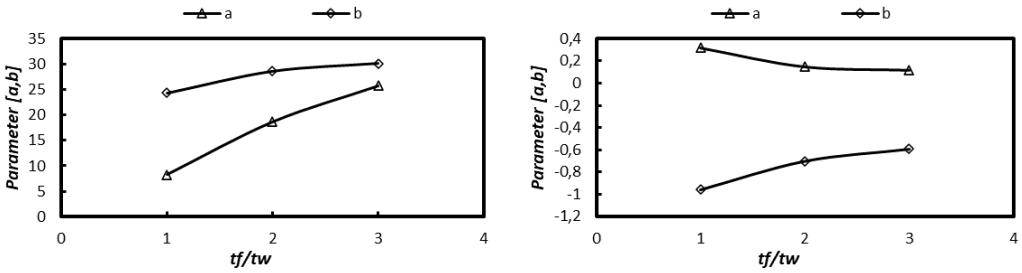

Figure 24: *a* and *b* in terms of t_f/t_w for horizontal position.

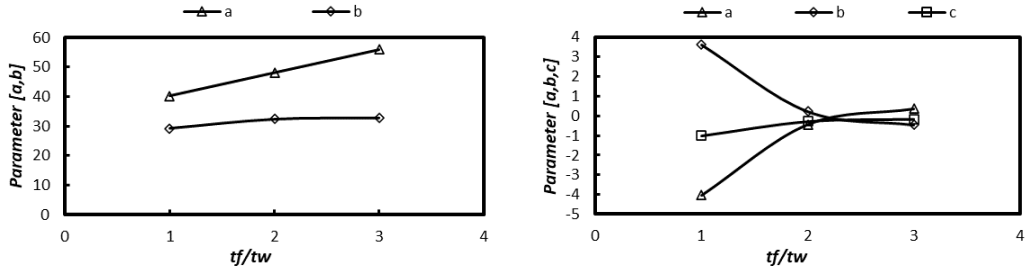

Figure 25: *a* and *b* in terms of t_f/t_w for inclined position.

8. In a hierarchical way, the equation proposed in 3) was rewritten with steps 4) and 5), in order to obtain the final equations.

Mid-Height:

$$k_s = \left[\left(20.8 \cdot \frac{t_f}{t_w} + 2.4\right) \cdot tan\theta + 1.8 \cdot \frac{t_f}{t_w} + 26\right] \cdot \left(\frac{a}{h_0}\right)^{\left[\left(-0.2 \cdot \frac{t_f}{t_w} + 0.5\right) \cdot tan\theta + 0.2 \cdot \frac{t_f}{t_w} - 1.1\right]} \quad (5)$$

Horizontal:

$$k_s = 0.95 \cdot \left[\left(8.7 \cdot \frac{t_f}{t_w} + 0.1\right) \cdot tan\theta + 2.9 \cdot \frac{t_f}{t_w} + 22\right] \left(\frac{a}{h_0}\right)^{\left[\left(-0.1 \cdot \frac{t_f}{t_w} + 0.4\right) \cdot tan\theta + 0.2 \cdot \frac{t_f}{t_w} - 1.1\right]} \quad (6)$$

Inclined:

$$k_s = \left[\left(7.9 \cdot \frac{t_f}{t_w} + 32.4\right) \cdot tan\theta + 1.8 \cdot \frac{t_f}{t_w} + 28\right] \cdot \left(\frac{a}{h_0}\right)^{(-0.29)} \quad (7)$$

4.2 Statistical evaluation

Fig. 26 shows the correlation between the computed buckling coefficient and those obtained with Eqs. (5), (6) and (7). It can be seen that the best correlation is attained for the girder stiffened at mid-height with R^2=0.99, for the stiffener placed horizontally R^2=0.95, and finally for the stiffener placed parallel to the inclined flange R^2=0.91.

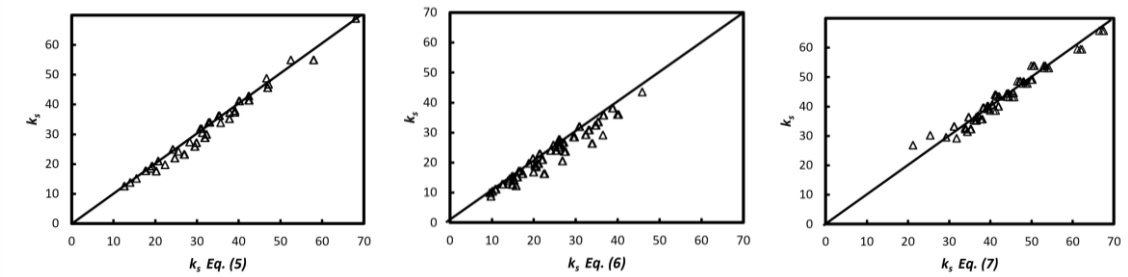

(a) Eq. (5) - R^2=0.99 (b) Eq. (6) - R^2=0.91 (c) Eq. (7) - R^2=0.95

Figure 26. Correlation between numerical results and proposed formulas

5. Conclusions

In this paper, the critical buckling response of longitudinally stiffened-haunched steel plate girders subjected to shear loading was investigated through finite elements analysis. An extensive parametric study was performed varying the panel aspect ratio, the flange-to-thickness ratio, the stiffener rigidity and location (mid height, horizontal and inclined). From the results the following conclusion are drawn:

.- The use of longitudinal stiffeners increases the critical buckling coefficient k_s, and hence the critical stresses, of haunched girders subjected to shear loading.

.- Among the investigated parameters, the slenderness of the panel h_1/t_w has a negligible impact on the buckling coefficients.

.- Regarding the flexural rigidity of the stiffener, within the range of parameters evaluated herein there is a diminished influence for $\gamma_s \geq 20$. Beyond this limit, buckling of the webpanel is divided into two subpanels, and the whole girder attains a greater buckling load. The highest buckling coefficients were attained when the longitudinal stiffener was located parallel to the inclined flange.

.-Locating the stiffener parallel to the inclined flange works the best.

.- Buckling coefficients calculated with the proposed formulas attained very high correlation with the values computed numerically.

References

AASHTO (2020). AASHTO LRFD Bridge Design Specifications. 9th Edition, American Association of State Highway and Transportation Officials, Washington, DC.

ANSYS. Ansys Release 2022 R1

AbdelAleem, B.H., Ismail, M.K., Haggag, M., El-Dakhakhni, W., Hassan, A.A. (2022). "Interpretable soft computing predictions of elastic shear buckling in tapered steel plate girders." *Thin-Walled Structures*, 176, 109313.

Bedynek, A., Real, E., Mirambell, E. (2013). "Tapered plate girders under shear: Tests and numerical research." *Engineering Structures*, 46, 350-358.

Bedynek, A.E., Mirambell, E. (2013). "Shear buckling coefficient for simply-supported tapered plates subjected to shear." *Proceedings of the Institution of Civil Engineers – Structures and Buildings*; 166.

Bedynek, A., Mirambell, E., Real, E. (2013). "Experimental and numerical research on longitudinally stiffened tapered steel plate girders subjected to shear." *In Research and Applications in Structural Engineering, Mechanics and Computation* (pp. 459-460). CRC Press.

Bedynek, A. "Structural behaviour of tapered steel plate girders subjected to shear." Doctoral Dissertation, Construction Engineering Department, Universitat Politécnica de Catalunya, 2014. Available at: <http://hdl.handle.net/2117/95340>.

Bedynek, A., Real, E., Mirambell, E. (2014) "Shear buckling coefficient: proposal for tapered steel plates." *Proceedings of the Institution of Civil Engineers - Structures and Buildings* 167(4): 243-252.

Bedynek, A., Real, E., Mirambell, E. (2017). "Design proposal for ultimate shear strength of tapered steel plate girders." *Informes de la Construcción*, 69(545), 1-12.

Eurocode 1993-1-5: Eurocode 3 (EC3): Design of Steel Structures – Part 1-5. 2006.
Hassanein, M.F., Kharoob, O.F. (2014). "Shear buckling behavior of tapered bridge girders with steel corrugated webs." *Engineering Structures*, 74, 157-169.
Hassanein, M.F., Kharoob, O.F. (2015). "Linearly tapered bridge girder panels with steel corrugated webs near intermediate supports of continuous bridges." *Thin-Walled Structures*, 88, 119-128.
Ibrahim, M.M., El-Aghoury, I.M., Ibrahim, S.A.B. (2020). "Finite element investigation on plate buckling coefficients of tapered steel members web plates." *Structures*, 28, 2321-2334).
Ibrahim, M.M., El Aghoury, I.M., Ibrahim, S.A.B. (2020). "Experimental and numerical investigation of ultimate shear strength of unstiffened slender web-tapered steel members." *Thin-Walled Structures*, 148, 106601.
Kuhlmann, U., Breunig, S., Gölz, L.M., Pourostad, V., Stempniewski, L. (2020). "New developments in steel and composite bridges." *Journal of Constructional Steel Research*, 174, 106277.
Mirambell, E., Zárate, V. (2000). "Web buckling of tapered plate girders." *Proceedings of the Institution of Civil Engineers - Structures and Buildings*, 140(1), 51-60.
Pourostad, V., Kuhlmann, U. (2018). "Experimental investigations on girders with non-rectangular panels". *Eighth International Conference on Thin-Walled Structures - ICTWS 2018*, Lisbon, Portugal.
Pourostad, V., Kuhlmann, U. (2019). "Experimental and numerical investigations of unstiffened steel girders with non-rectangular panels subjected to bending and shear." *The International Colloquium on Stability and Ductility of Steel Structures - SDSS 2019*, Prague, Czech.
Pourostad, V., Kuhlmann, U. (2021). "New development of design rules for girder with non-rectangular slender web." *ce/papers*, 4(2-4), 1797-1804.
Real, E., Bedynek, A., Mirambell, E. (2010). "Numerical and experimental research in tapered steel plate girders subjected to shear." *Proceedings of SDSS'Rio 2010: International Colloquium Stability and Ductility of Steel Structures*, Rio de Janeiro, Brazil, 747-754.
Sediek, O.A., Safar, S.S., Hassan, M.M. (2020). "Numerical investigation on shear strength of tapered perfect end web panels." *Structures*, 28, 354-368.
Timoshenko S.P., Gere J.M. (1936). Theory of elastic stability. Courier Corporation.
Zárate AV, Mirambell, E. (2004). "Shear strength of tapered steel plate girders." *Proceedings of the Institution of Civil Engineers – Structures and Buildings*, 157(5), 343-54.
Zevallos, E., Hassanein, M.F., Real, E., Mirambell, E. (2016). "Shear evaluation of tapered bridge girder panels with steel corrugated webs near the supports of continuous bridges." *Engineering Structures*, 113, 149-159.
Ziemian, R. D. (Ed.). (2010). Guide to stability design criteria for metal structures. John Wiley & Sons.